# NATIONAL ADVISORY COMMITTEE
# FOR AERONAUTICS

**TECHNICAL NOTE 2220**

A BALSA-DUST TECHNIQUE FOR AIR-FLOW VISUALIZATION

AND ITS APPLICATION TO FLOW THROUGH MODEL

HELICOPTER ROTORS IN STATIC THRUST

By Marion K. Taylor

Langley Aeronautical Laboratory
Langley Air Force Base, Va.

NACA

Washington
November 1950
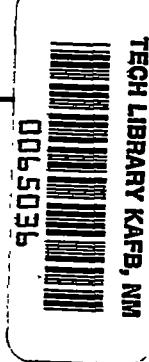
1.

NATIONAL ADVISORY COMMITTEE FOR AERONAUT

TECHNICAL NOTE 2220

A BALSA-DUST TECHNIQUE FOR AIR-FLOW VISUALIZATION

AND ITS APPLICATION TO FLOW THROUGH MODEL

HELICOPTER ROTORS IN STATIC THRUST

By Marion K. Taylor

## SUMMARY

A method of visualizing air-flow patterns by observing the motion of finely divided particles of balsa wood introduced into the air has been developed by the National Advisory Committee for Aeronautics. The technique is simple to use and requires only a supply of balsa wood, a camera, and photographic lamps. Photographic results obtained by this method for small-scale models of several helicopter rotor configurations in the static-thrust condition are presented. The results indicate the feasibility of using the NACA balsa-dust technique for obtaining useful qualitative information on the air-flow patterns for transient conditions as well as for steady-state conditions.

## INTRODUCTION

The trend toward increasing the size and load capacity of heli-copters has resulted in increased use of multiple-rotor configurations. A general investigation of multiple-rotor configurations is therefore being conducted in the Langley full-scale tunnel. In order to supple-ment the full-scale data, information on the air-flow patterns through small-scale rotors was considered desirable. A method was consequently devised for visualizing the air flow through use of balsa-dust particles, designated hereinafter the NACA balsa-dust technique. This method has provided a simple means of observing the flow distribution through model rotors and is suited for many other applications in which a pictorial representation of the air-flow pattern in a given plane is desired. Since the first multiple-rotor arrangement in the full-scale-tunnel program is a coaxial system, a coaxial model having a diameter 1/15 that of the full-scale rotor was constructed. This scale was chosen to permit an investigation of the flow patterns in various forward-flight condi-tions in the $\frac{1}{15}$ - scale model of the Langley full-scale tunnel.

In this paper, only the results obtained for the rotor in the
static-thrust condition are presented.  The information was obtained
from still photographs and motion pictures and includes, for comparison
purposes, the results obtained with one of the rotors removed from the
coaxial-model configuration.  The effect of placing a ground plane at
several distances from the rotor and the air-flow distribution resulting
from a rapid increase in rotor thrust were investigated.  No quantitative
analysis of the data is made, but certain flow phenomena shown make
possible some general observations regarding the influence of flow con-
ditions on rotor characteristics.  Limited studies were also made with
a biaxial helicopter model.

## NACA BALSA-DUST TECHNIQUE OF FLOW VISUALIZATION

Several years ago, when a graphic qualitative record of the flow
pattern of a helicopter rotor in various flight conditions was desired,
a number of indicating materials, including smoke, were tested.  Finely
divided balsa-wood particles were found to provide the best combination
of high reflectivity and low mass of any of the materials investigated.
Inasmuch as the information on this technique has not been previously
published, a detailed description of the method is considered worth
while.  This balsa-dust method of air-flow visualization is simple to
use and requires only a supply of balsa wood, a camera, and photographic
lamps.

The balsa dust was made from select grade 1 balsa wood by sanding
it across the grain on a belt sander using a fine grade of sandpaper.
The dust thus produced was then sifted twice through 18-mesh screen.
The resulting product had an average free-fall velocity in air of approxi-
mately 1 foot per second, although some of the grains were so fine that
they hung almost motionless in the air.

A narrow trough 8 feet long, having a screened bottom, was mounted
approximately 4 feet above the rotor and filled with this balsa dust.
A mechanical shaker provided the motion necessary for introducing the
dust into the air above the rotor.  The dust was visualized by projecting
a narrow beam of high-intensity light perpendicular to the viewing axis.
The light source consisted of two 2000-watt Solar spotlights and ten
250-watt fixed-focus spotlight lamps.  In some sequences, only the fixed-
focus spotlights were used.  Metal covers with narrow, parallel slits
served to define the light beam approximately 2 inches wide at the rotor
disk in a vertical plane.  This light was found to be adequate for taking
motion pictures at speeds up to 64 frames per second.  A standard 8-
by 10-inch plate camera and a 16-millimeter movie camera, which was
operated at 64 frames per second, were used to take still photographs

and motion pictures of the flow. During some of the tests, a motor-driven 35-millimeter motion-picture camera, operating at 48 frames per second, was also used to facilitate the making of enlargements of the photographs of the more interesting sequences. All three cameras were mounted to photograph the dust particles in the vertical light plane and were arranged to be operated simultaneously by the observer.

The shadows, seen in most of the photographs, are the result of structural interference with the criss-crossed light beams and could not be completely eliminated.

## ROTOR MODELS

The coaxial rotor model used in these studies is shown in figure 1. A small water-cooled three-phase electric motor supplied power to the counterrotating shafts through a conventional right-angle gear box. The rotational speed was obtained from a tachometer mounted on the drive-motor shaft. For this configuration and for the arrangement with one rotor removed, the rotor thrust was measured with an accuracy of approximately 10 percent by electric strain gages attached to the four thrust beams shown in figure 1.

The rotor model was of the two-blade see-saw type. The blades had an NACA 0012 airfoil section, no twist, a rectangular plan form, a solidity (per rotor) of 0.04, and were precision machined from solid duralumin. The rotor diameter was 20 inches. The rotor spacing in the coaxial configuration was 35 percent of the radius. Most of the tests were made at a rotational speed of 3842 rpm, which corresponded to a tip speed of 335 feet per second. The Reynolds number at the tip was approximately $1.1 \times 10^5$.

The biaxial model had two-blade see-saw type rotors of rectangular plan form, zero twist, and a solidity of 0.057. A Rhode St. Genese-35 airfoil section was used. This airfoil has a flat undersurface and a thickness ratio of 15 percent of the chord. The rotor diameter was 45 inches and the tests were made at a tip speed of 138 feet per second; this speed corresponded to a Reynolds number of $1.5 \times 10^5$. Provision was made for shortening the motor-drive shafts, which permitted rotor overlaps up to 85 percent of the radius to be obtained.

## TESTS

Photographs were obtained for the coaxial-rotor model and for the single-rotor configuration formed by removing the lower rotor over a

range of blade pitch settings. Observations were made with these two
configurations without a ground plane and in the presence of a ground
plane set at 25 percent and 50 percent of the rotor diameter below the
rotor. With the coaxial rotor the lower rotor was used as the reference
for the ground-plane setting.

The ground plane used in the studies of the coaxial-rotor and the
single-rotor configurations was 5 feet in diameter. Even with the
ground plane removed, however, some ground effect due to the rotor
supporting structure, which was located approximately 65 percent of the
rotor diameter below the lower rotor hub for the coaxial configuration,
was present.

Some flow data were also obtained for the single-and coaxial-rotor
model during rapid thrust increases, which were produced by rapidly
accelerating the rotor from rest up to a tip speed of 335 feet per second.

Limited observations with the biaxial-rotor system for configu-
rations with zero blade overlap and with the blades meshed 85 percent
of the radius were also made for the conditions with no ground plane
and with the ground plane set at 0.25 diameter below the rotor hubs.

PRESENTATION OF RESULTS

Single and coaxial rotors.- Typical photographs of the flow patterns
for the single-rotor arrangement without the ground plane and with the
ground plane set at 0.50 and 0.25 rotor diameters below the rotor are
shown in figures 2(a), 2(b), and 2(c). The average rotor-thrust coef-
ficient for these three conditions was approximately 0.0036. These
photographs were made with the view camera with an exposure of
1/5 second. Photographs obtained for similar conditions with the coaxial
configuration are presented in figures 3(a), 3(b), and 3(c). The rotor-
thrust coefficient for these coaxial tests was approximately 0.0060.
In general, the geometry of the air-flow pattern was not affected by the
magnitude of the rotor thrust coefficient. The large volume of air
above the rotor affected by the rotor, which is indicative of very small
induced velocities in this region, is shown in the photographs. For the
coaxial configuration, it is of interest to note that the vortex fila-
ments emanating from the blade tips of the upper and lower rotors do not
merge or cancel one another but retain their separate identities in the
wake. Some difficulty was experienced in obtaining a uniform distri-
bution of balsa dust within the field of view of the camera. This
distribution was especially inconsistent during the first few runs and
was greatly improved by manually shaking the trough.

Measurements of the flow geometry, as defined by the balsa-dust pattern in the photographs, were made by using each side of the photographs whenever possible in order to give the best average interpretation of the results. The wake of the single isolated rotor (fig. 2(a)), as indicated by the dark core of the tip vortex, is shown to contract to 75 percent of the rotor diameter at a distance 0.35 diameter below the rotor plane. Inasmuch as previously obtained photographs of an alternate single-rotor model supported on a long, slender shaft (fig. 4(a)) indicate that the wake contracts to a minimum diameter of 0.70 diameter at a distance of approximately one radius below the rotor plane, some interference on the wake because of the rotor-supporting structure for the condition with no ground plane must be present. With the ground plane in place, however, this source of error is removed, and a comparison of the flow patterns obtained on these two single-rotor models at a ground-plane setting of 0.25 diameter are in fairly good agreement. (See figs. 2(c) and 4(b).)

Measurements of the location and magnitude of the minimum wake diameter for the three rotors shown in figures 2 to 4 have been obtained from the photographs and are shown plotted as a function of ground-plane location in figure 5. For convenience, the results obtained without the ground plane have been plotted at a ground-plane distance of one rotor diameter. This assumption is believed to be justified inasmuch as the ground effect is negligible for distances of one rotor diameter or more. The presence of the ground plane broadens the minimum wake area and locates this area approximately one-third of the distance down from the plane of the rotor to the ground plane. The blade-tip vortex patterns for the upper and lower rotors of the coaxial configuration bracket the pattern obtained for the single-rotor arrangement due to mutual interference effects. The photographs of the coaxial rotor indicate that the slipstream of the upper rotor may have to be considered in theoretical calculations involving the lower rotor, particularly in stress analysis work since the nonuniformity of the downwash field may result in large bending-moment differences between the two rotors.

An interesting flow instability was observed in studies of the single rotor made with the ground plane set at 0.25 diameter. As intercepted by the light plane, a small area of rotation centered at one blade root gradually enlarged, moved radially and down from the rotor, and finally was swept out from under the rotor disk. The same type of flow, though out of phase, occurred on the opposite side of the rotor. This unstable flow occurred simultaneously with a slight rocking motion of the rotor about the flapping hinge. These motions are much too periodic to be caused by stray air currents and appear to be peculiar to this model, inasmuch as they had not been noticed on other single-rotor models studied previously. This flow instability may be seen in figure 2(c) (see insert) and is centered on the left side of the rotor disk at approximately 40 percent of the blade span. Several plausible

explanations of this phenomenon have been investigated but have not
provided a satisfactory answer. This type of flow is not present at
ground-plane settings greater than 0.25 diameter.

Biaxial rotor.- Although the biaxial model was considered too large
for the testing facilities, an investigation of the flow pattern for any
unusual trends was considered desirable before plans were made to con-
struct a suitable model for more extensive flow visualization purposes.
Because of the relatively large size of the biaxial model, the dust
trough and ground plane were located to show a complete flow pattern for
one rotor. Figures 6(a) and 6(b) present photographs of the biaxial
model with zero overlap in the presence of a ground plane set at
0.25 diameter and with the ground plane removed. Figures 7(a) and 7(b)
show the rotor blades meshed 85 percent of the radius for similar ground-
plane conditions.

No unusual trends are present with the ground plane removed. The
most interesting flow patterns observed with this model, however,
occurred in the presence of the ground plane. In figure 6(b), a strong
tendency for the flow which passed through the center of the swept area
to recirculate through each rotor in the vicinity of the hub can be
noticed. Meshing the rotors 85 percent of the radius at the same ground-
plane and blade-pitch settings appreciably reduced the recirculation
because of the influence of the tip-vortex filaments of the meshing
blades (fig. 7(b)). A sketch of the air-flow patterns visualized for
the biaxial rotor in the presence of the ground plane is included as
figure 8.

Rapid thrust increase.- Photographs were also taken of the flow
patterns during a rapid thrust increase. Inasmuch as the collective
pitch could not be changed during a run, the rapid thrust increase was
obtained by rapidly accelerating the rotor from rest. The resulting
flow patterns for the single rotor (fig. 9) are strikingly similar to
those obtained in a similar investigation on the Langley helicopter test
tower in which smoke streamers were used for visualization purposes, and
in which the sudden thrust increase was obtained by a rapid change of
pitch instead of by a rapid increase in angular velocity.

The photographs included in figure 9 show that the large vortex
associated with the thrust increase is quickly generated by the indi-
vidual blade-tip vortex filaments and is rapidly carried downstream as
the rotor induced velocity builds up to its normal value. With the
coaxial rotors (fig. 10), the filaments from the upper and lower rotors
join to form a starting vortex similar to that seen in the single-rotor
starts.

# CONCLUSIONS

The NACA balsa-dust technique of air-flow visualization has been used to obtain air-flow patterns through model helicopter rotors operating in static thrust in both steady-state and transient-flow conditions. This balsa-dust technique is simple to apply and requires no specialized equipment. The following conclusions may be drawn as a result of this investigation:

1. In a coaxial configuration the blade-tip vortex patterns obtained for the upper and lower rotors remain separate in the wake and approximately bracket the vortex pattern obtained for a single rotor.

2. The slipstream of the upper rotor in the coaxial configuration may be a factor in producing rotor-blade bending moments in the lower rotor.

3. The recirculation of the wake in the vicinity of the rotor hub, noticed for the biaxial rotor without overlap and in the presence of a ground plane set at 0.25 diameter, was greatly reduced by meshing the blades 0.85 radius.

Langley Aeronautical Laboratory
        National Advisory Committee for Aeronautics
                Langley Air Force Base, Va., September 1, 1950.

Thrust beams

Drive motor

Gear box

Cradle

Tachometer

Support box
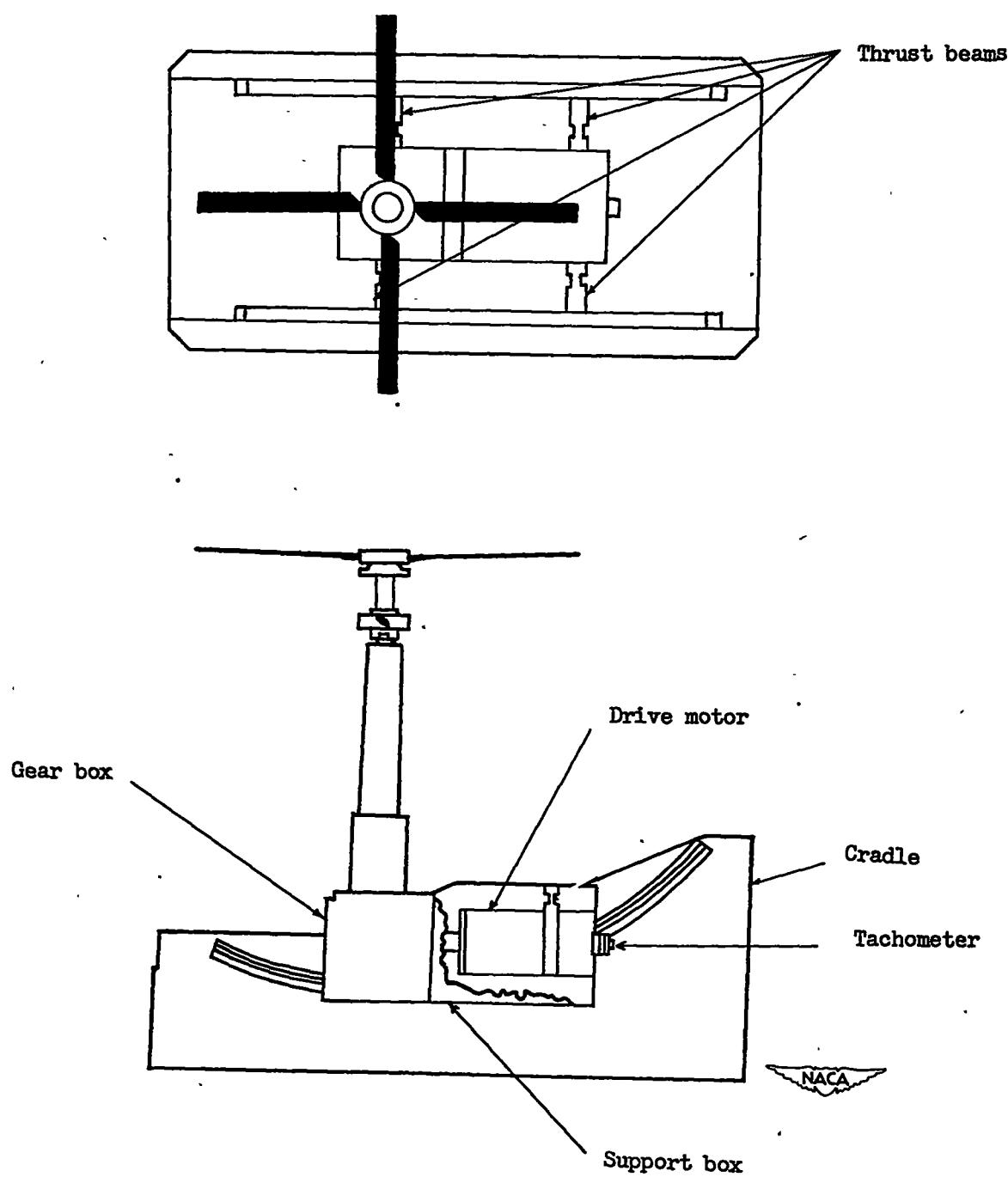
Figure 1.- Schematic diagram of the coaxial rotor model.
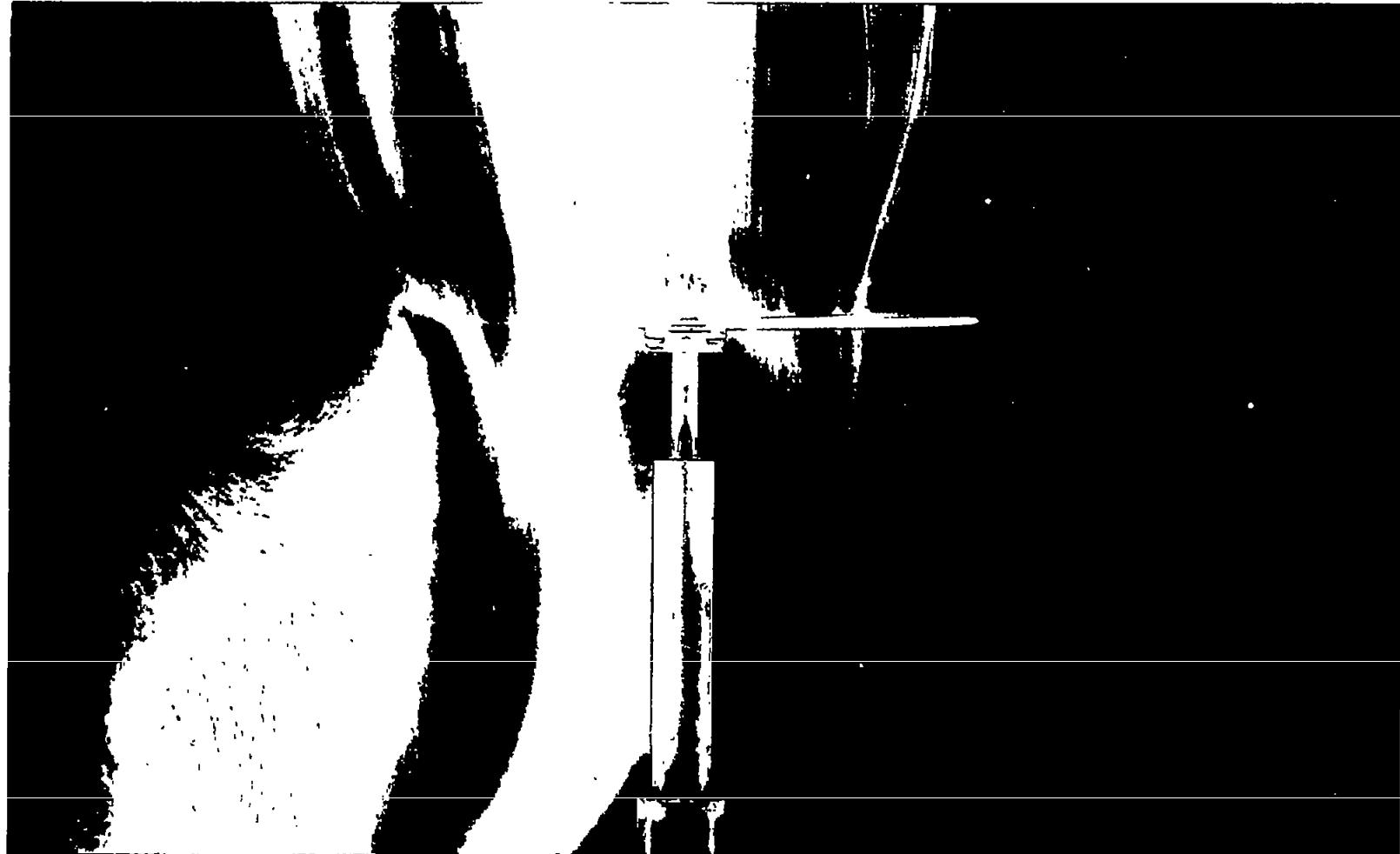
(a) No ground plane.
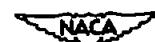
L-62796

Figure 2.- Single-rotor arrangement in the static-thrust condition. Approximate rotor-thrust coefficient of 0.0036.

(b) Ground plane at 0.50 diameter.

Figure 2.- Continued.

L-66044

(c) Ground plane at 0.25 diameter.

Figure 2.- Concluded.
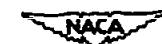
L-65028.1
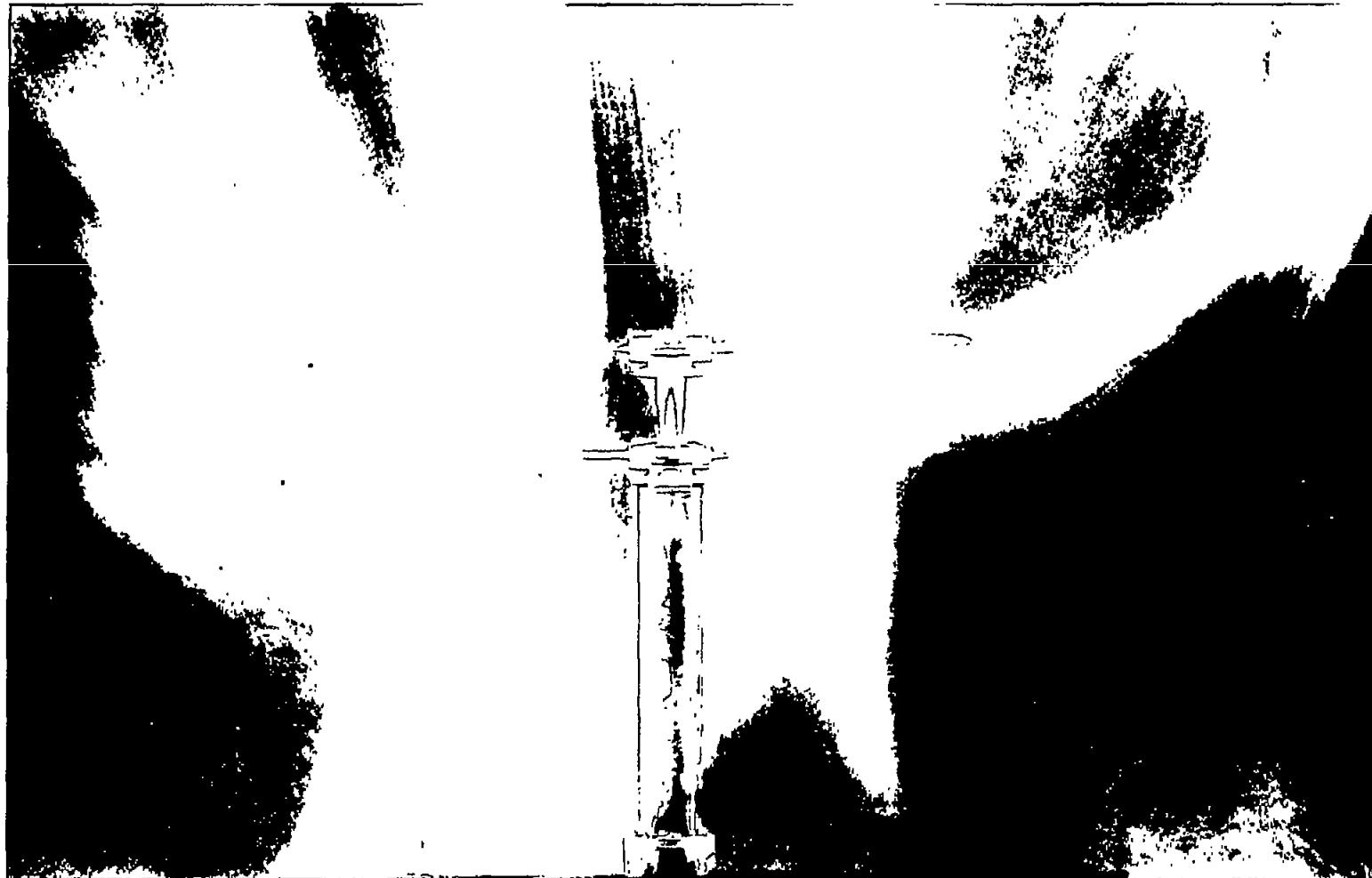
(a) No ground plane.

L-65027

Figure 3.- Coaxial rotor in the static-thrust condition.  Approximate
rotor-thrust coefficient of 0.0060.

(b) Ground plane at 0.50 diameter.

Figure 3.- Continued.

L-66043

(c) Ground plane at 0.25 diameter.

Figure 3.- Concluded.

L-65026
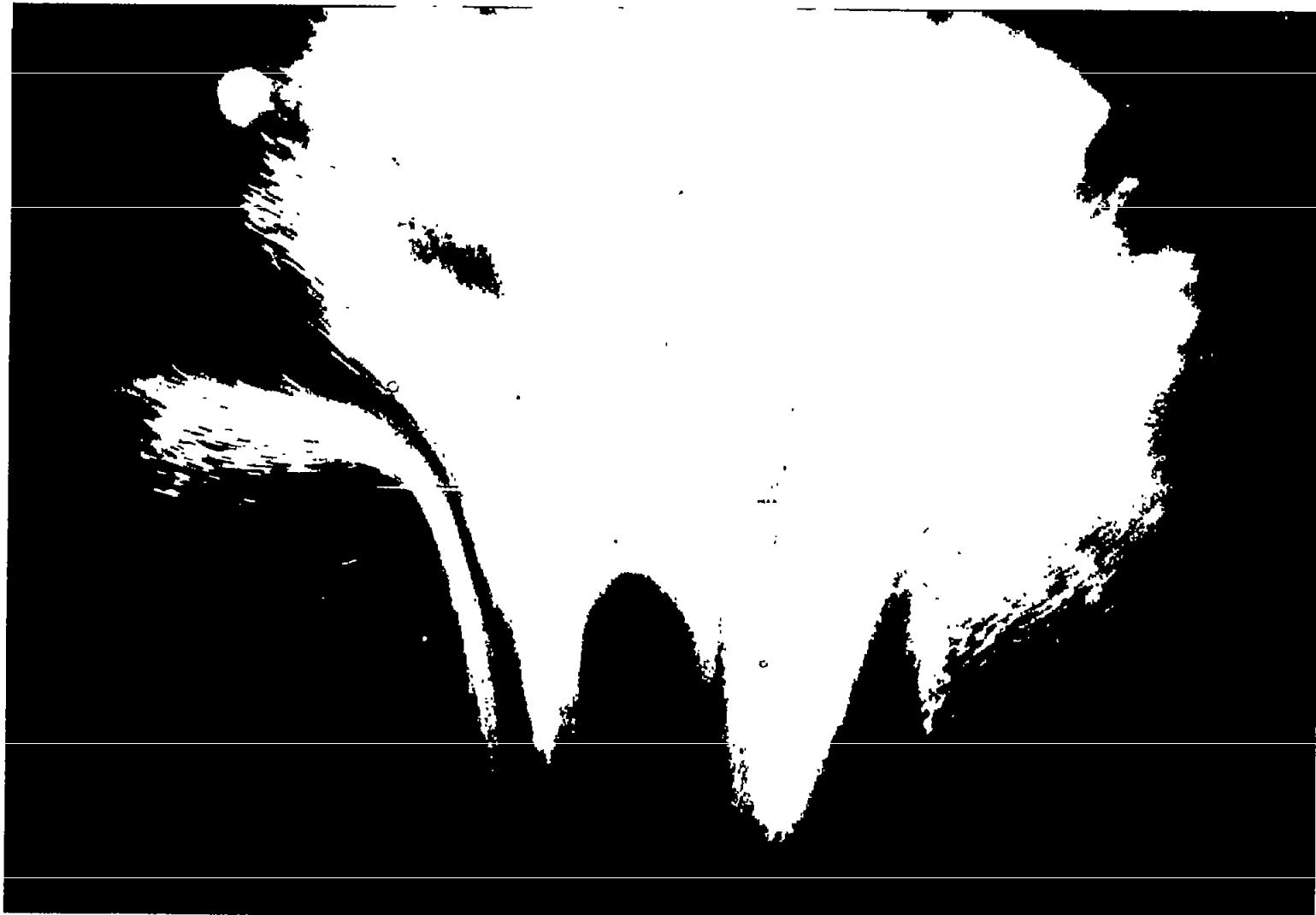
(a) No ground plane.

L-46819

Figure 4.- Alternate single rotor in the static-thrust condition.
Approximate rotor-thrust coefficient of 0.0044.

(b) Ground plane at 0.25 diameter.

Figure 4.- Concluded.

L-47245

———O— Single-rotor arrangement
——— ———□— Coaxial configuration:  upper rotor
——— ——◇— Coaxial configuration:  lower rotor
        △    Check points for alternate single rotor
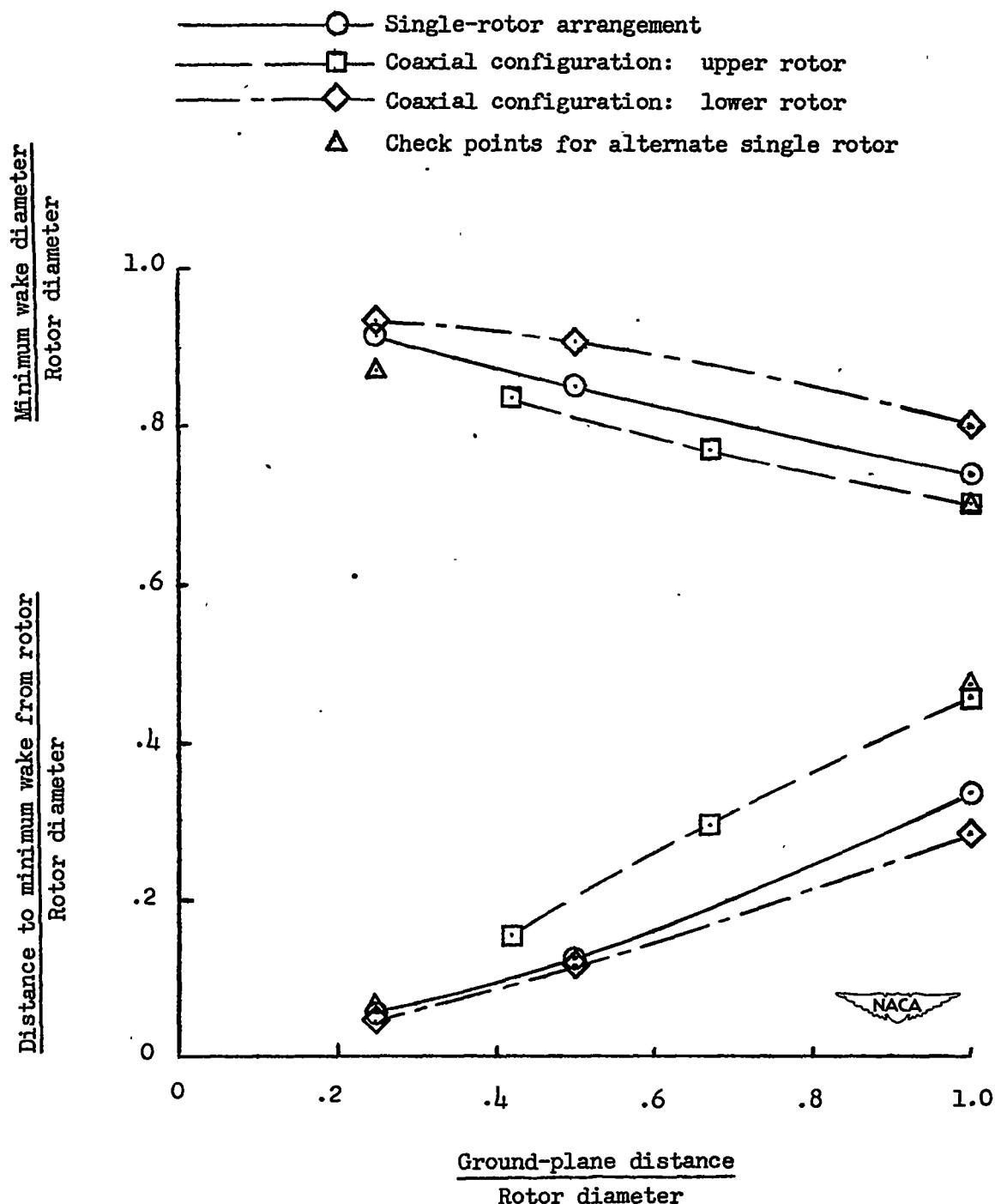


Figure 5.- Rotor-wake characteristics obtained from figures 2 to 4.

(a) No ground plane.
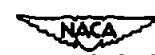
L-66046

Figure 6.- Biaxial rotor with zero overlap. Blade pitch approximately 17°.

(b) Ground plane at 0.25 diameter.

Figure 6.- Concluded.

L-66045

(a) No ground plane.
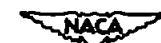
L-66047

Figure 7.- Biaxial rotor with 0.85-radius overlap. Blade pitch
approximately 17°.
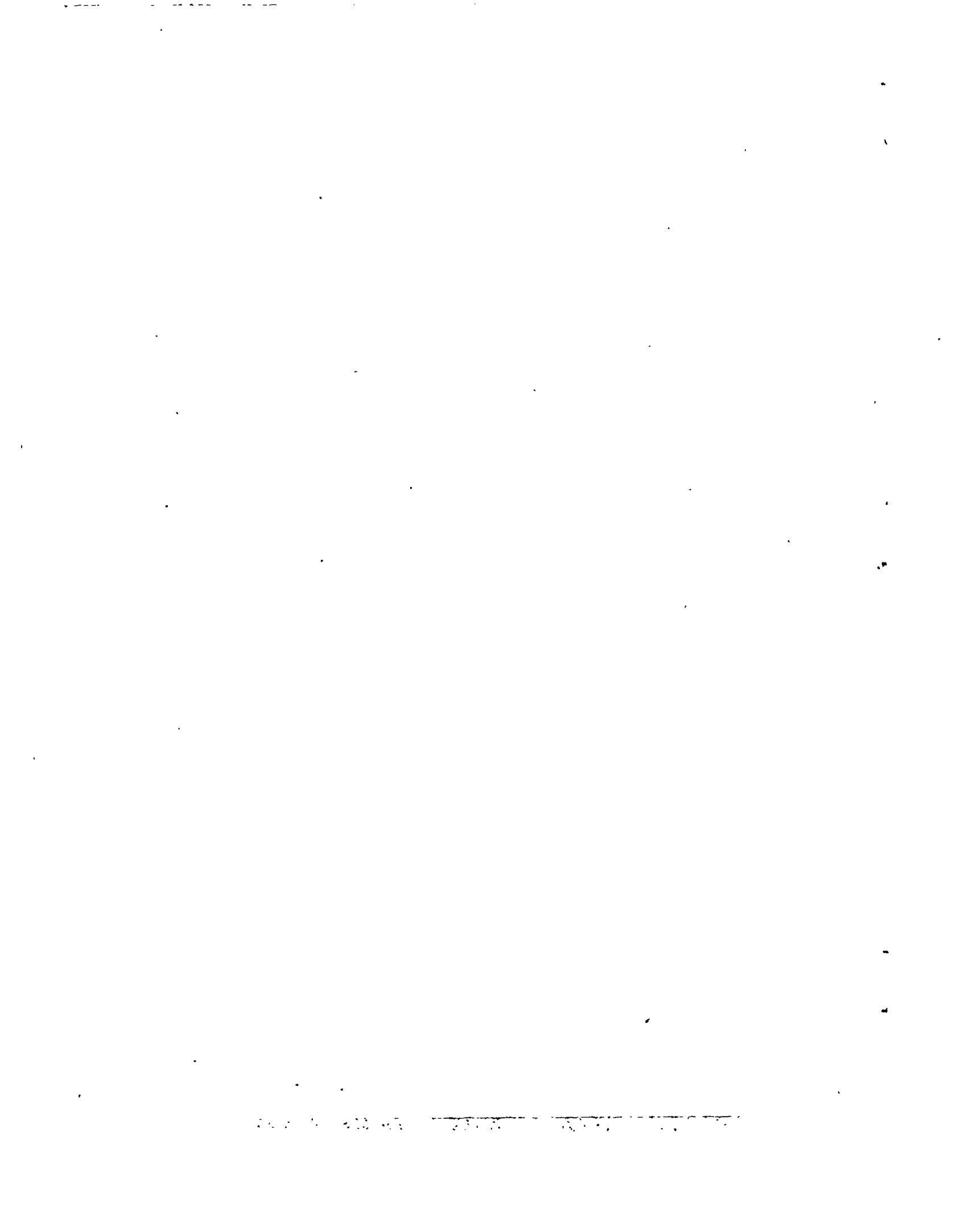
(b) Ground plane at 0.25 diameter.

Figure 7.- Concluded.

L-66508
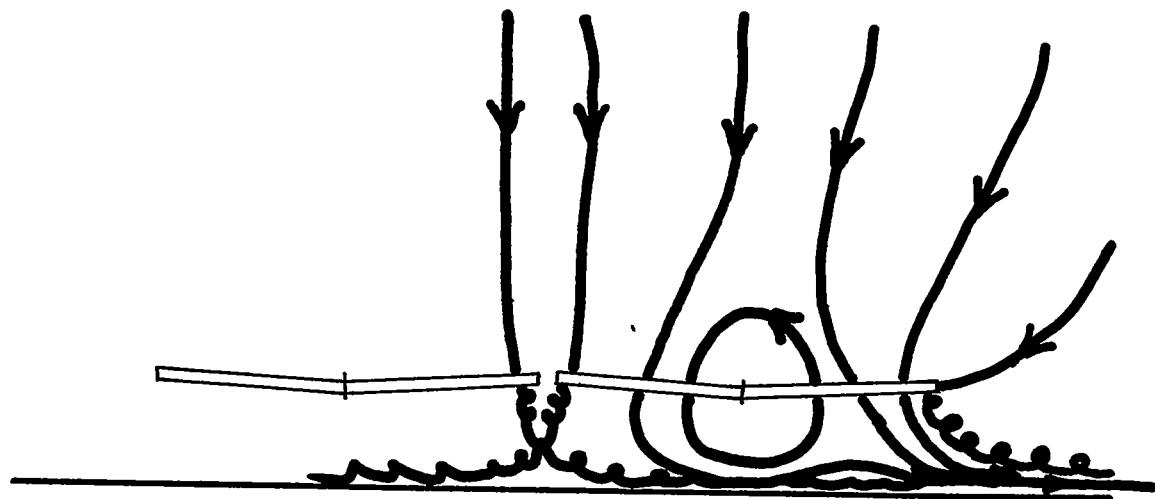
(a) Zero overlap.
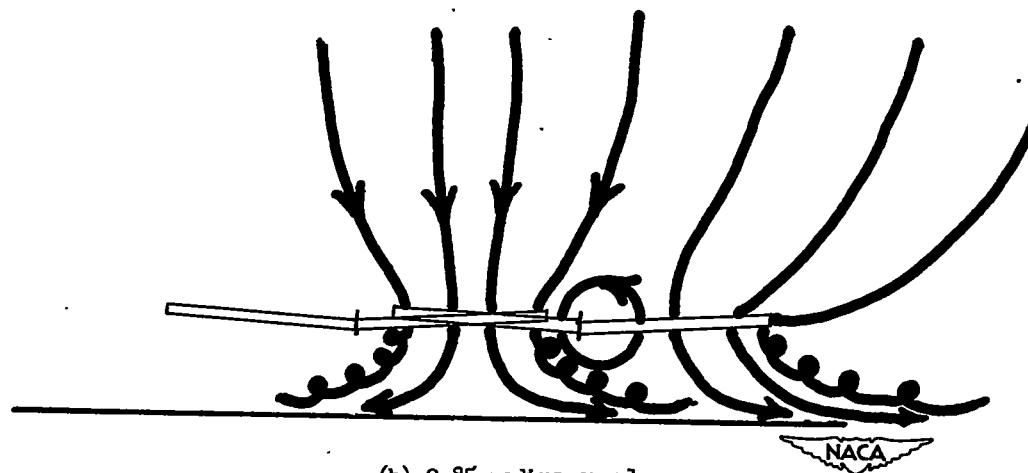


(b) 0.85 radius overlap.

Figure 8.- Schematic diagram of air-flow pattern through biaxial rotor.
Ground plane at 0.25 diameter.

Figure 9.- Single-rotor sudden-start sequence. Steady-state rotor-
thrust coefficient approximately 0.0046.

L-62471
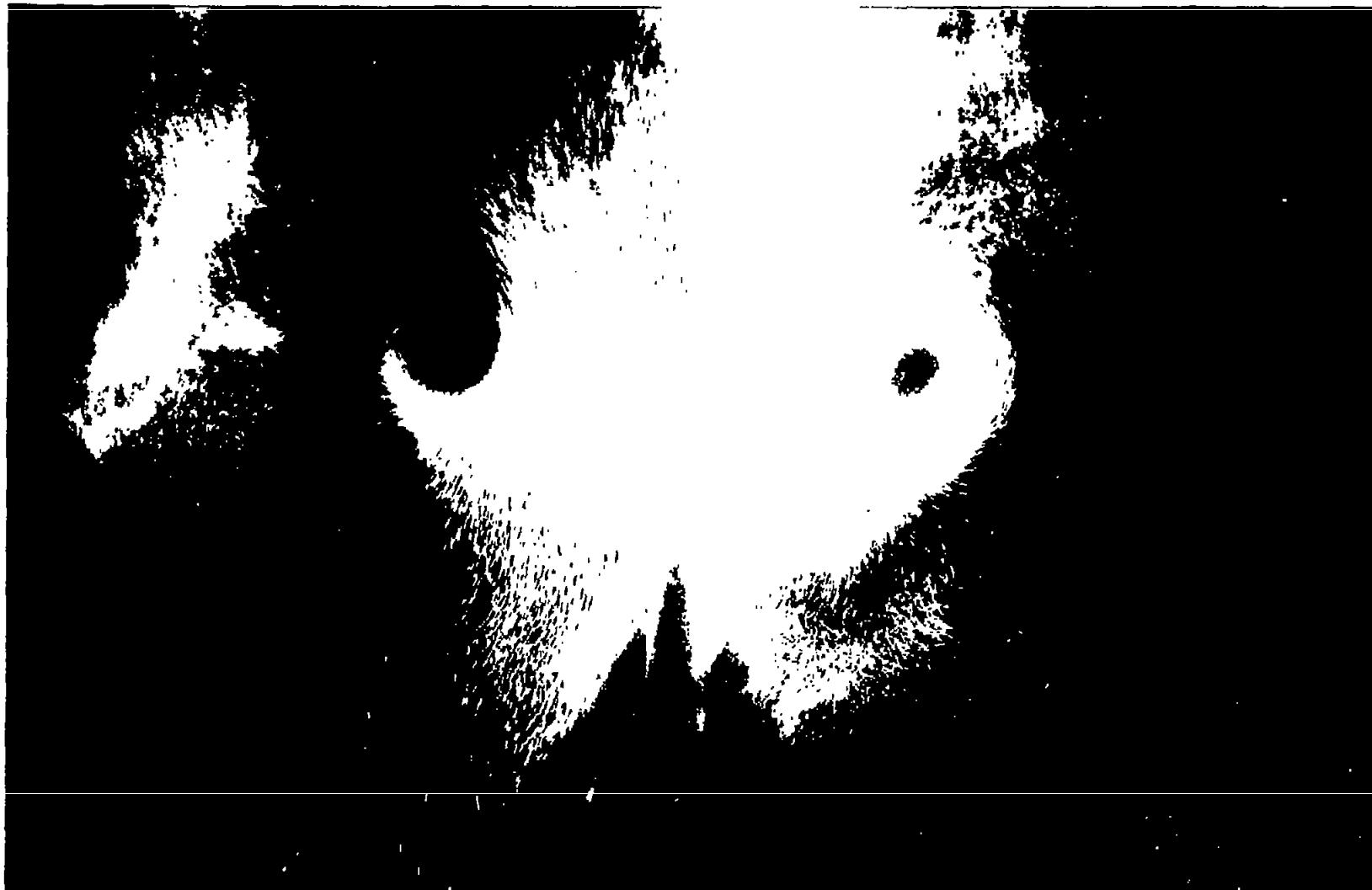
Figure 9.- Continued.
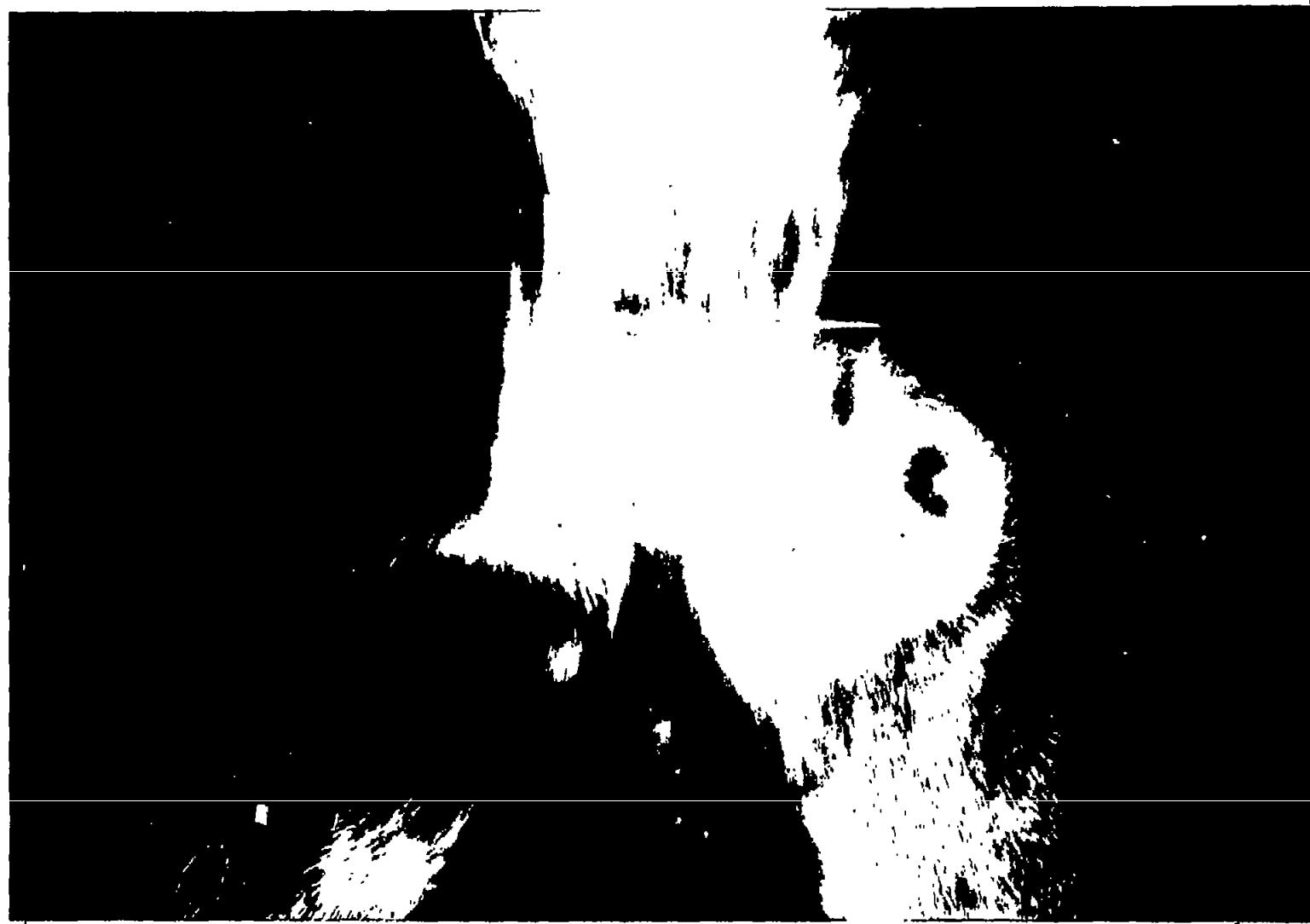
L-62463

Figure 9.- Concluded.

L-62464

41
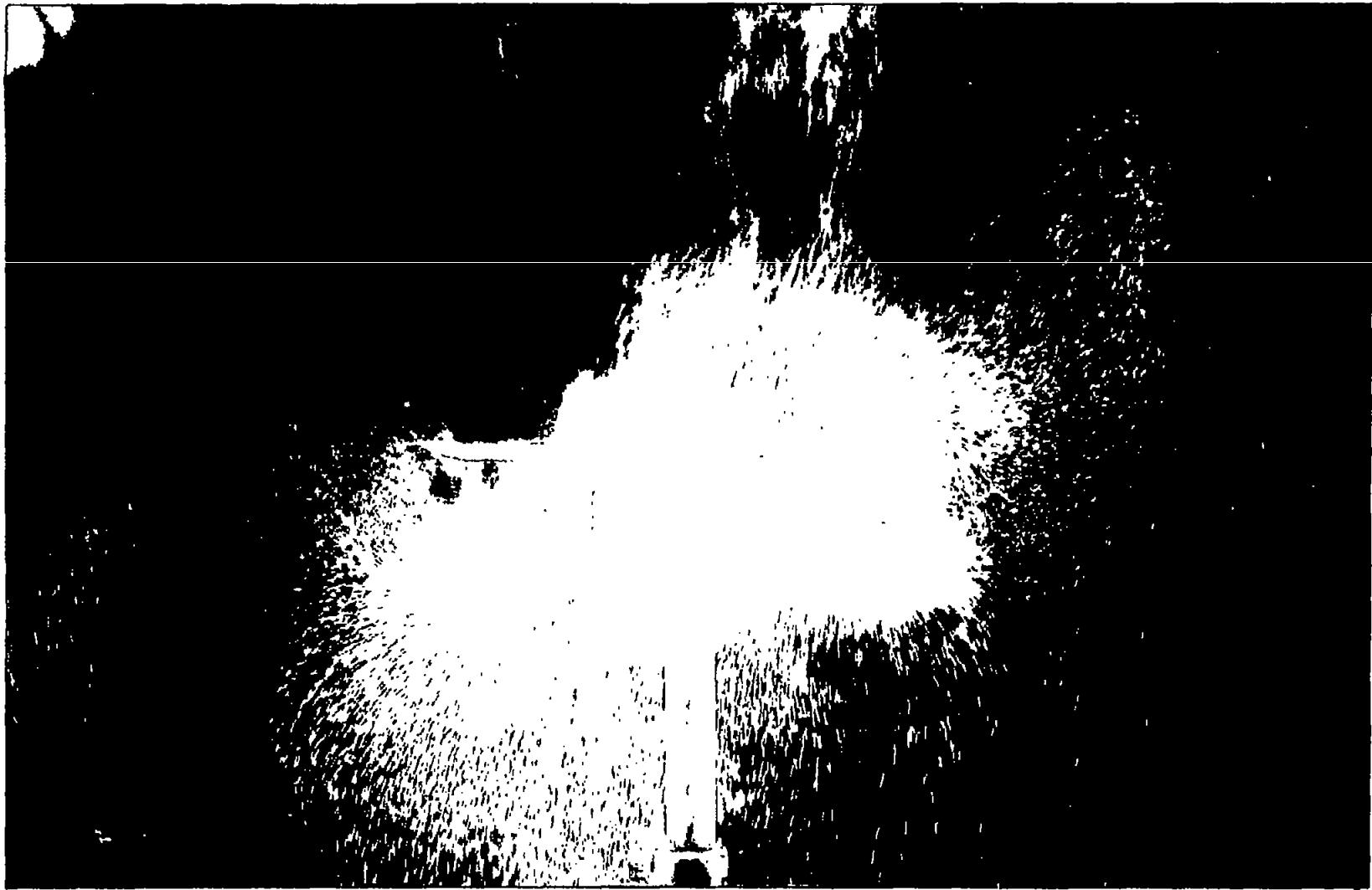
Figure 10.- Coaxial-rotor sudden-start sequence. Steady-state rotor-
thrust coefficient approximately 0.0088.

L-60741

Figure 10.- Continued.

L-60751